A parameterisation of the soot aging for global climate models

N. Riemer, H. Vogel, B. Vogel

Atmos. Chem. Phys. Discuss., 4, 2089–2115, 2004
www.atmos-chem-phys.org/acpd/4/2089/
SRef-ID: 1680-7375/acpd/2004-4-2089

Atmospheric Chemistry and Physics Discussions

A parameterisation of the soot aging for global climate models

N. Riemer[1], **H. Vogel**[1], **and B. Vogel**[2]

[1]Department of Mechanical and Aeronautical Engineering, University of California, Davis, USA
[2]Institut für Meteorologie und Klimaforschung, Forschungszentrum Karlsruhe, Karlsruhe, Germany

Received: 2 March 2004 – Accepted: 29 March 2004 – Published: 16 April 2004

Correspondence to: B. Vogel (bernhard.vogel@imk.fzk.de)

Abstract

The representation of soot in global climate models is desirable since it contributes to both the direct and indirect climate effect. While freshly emitted soot is initially hydrophobic and externally mixed, it can be transferred into an internal mixture by coagulation, condensation or photochemical processes. These aging processes affect the hygroscopic qualities and hence the growth behaviour, the optical properties and eventually the lifetime of the soot particles. However, due to computational limits the aging of soot in global climate models is often only parameterised by an estimated turnover rate resulting in a lifetime of soot of several days. Based on the results of our simulations with a comprehensive mesoscale model, we derive the timescale on which diesel soot is transferred from an external to internal mixture, and propose a parameterisation for the use in global climate models. This parameterisation is applicable to continental conditions in industrialised areas as can be found in Central Europe and North America. For daytime conditions, away from the sources, condensation is dominant and the aging process occurs very fast with a timescale of τ=2 h. During night time condensation is not effective. Then coagulation is the most important aging process and our parameterisation leads to a timescale between 10 h and 40 h.

1. Introduction

Soot particles are an important constituent of the atmospheric aerosol, since they participate in tropospheric chemistry (Saathoff et al., 2001), affect human pulmonary health (Pope and Dockery, 1996) and scatter and absorb light (Horvath, 1993). The size distribution of soot particles peaks in the accumulation range, therefore dry deposition velocities are small and soot particles can attain long lifetimes and be transported over long distances. The source of soot particles is the incomplete combustion of carbon containing material, which means that except for natural biomass burning all sources of soot are anthropogenic. In cities of the northern hemisphere the combus-

ACPD

4, 2089–2115, 2004

tion of fossil fuel dominates the sources. Typical concentrations of soot range between several hundreds of nanograms per m^3 in unpolluted areas to several micrograms per cubic meter in urban regions (Heintzenberg, 1988; Brémond, 1989; Baltensperger et al., 2002). While freshly emitted soot particles are hydrophobic and present in an external mixture their hygroscopic qualities can change due to the coagulation with soluble aerosols, condensation, and photochemical processes (Weingartner et al., 1997). Hereby the particle growth in response to ambient relative humidity, the optical properties, and the ability of being activated as cloud condensation nuclei are determined. Measurements show that both the external and the internal mixing state exist in the atmosphere (Okada, 2001) and that the hydrophobic portion of the aerosols decreases significantly as the distance from the sources increases.

It is well recognized that soot particles contribute to both the direct and indirect climate effect. While Lesins et al. (2002) and Jacobson (2000) recently studied the direct effect Nenes et al. (2002) highlighted the indirect effect. A number of studies in the past have been devoted to the representation of soot in global scale models (Liousse et al., 1996; Cooke et al., 1996, 1999; Lohmann et al., 2000) and the impact of soot aerosol on global climate (Jacobson, 2002).

However, due to computational limits the aging of soot in global scale models is often not represented explicitly but parameterised. For example, Liousse (1996) assume that soot is hydrophilic as soon as it is emitted. Myhre et al. (1998), in contrast, hypothesize soot to be hydrophobic. Tsigaridis and Kanakidou (2003) assume that the aging process occurs due to photochemical reactions. Cooke et al. (1996) parameterize the aging process by an estimated turnover rate of 1.25% h^{-1}, which translates to an exponential lifetime of 80 h. Lohmann et al. (2000) assume an exponential lifetime of 40 h emphasizing however, that the model results are highly sensitive to the turnover rate. Koch (2001) comes to a similar conclusion comparing three different methods for the parameterisation of the aging process.

Recently, Wilson et al. (2001) have provided a more detailed representation of the aging process in a global model. In their approach they explicitly calculate the aging of

ACPD
4, 2089–2115, 2004

soot depending on the abundance of sulphuric acid. Nevertheless, parameterisations of certain processes are still necessary when such global models are run in the climate mode, that is when several hundreds of years are simulated. We find it therefore worthwhile to carry out 3D simulations with the coupled mesoscale-γ model KAMM/DRAIS (Vogel et al., 1995) that provides a highly resolved boundary layer and allows for an explicit treatment of the aging process of soot by coagulation and condensation. The particle phase is treated with the aerosol model MADEsoot (Riemer et al., 2003) and calculates both the composition and the size distribution of the aerosol particles. Based on the results of our simulations, we derive the timescale on which soot is transferred from an external to an internal mixture, and thus calculate the turnover rates as would be used in a global climate model. In doing so, we focus on continental conditions in an industrialised environment and investigate two different meteorological scenarios, that is a summer and a winter episode.

2. Model description

The comprehensive model system KAMM/DRAIS couples the non-hydrostatic meteorological driver KAMM and the submodule DRAIS that calculates the transport and diffusion of the reactive trace gases and the aerosol particles. Since the model system KAMM/DRAIS has been described in detail in previous papers (Vogel et al., 1995; Hammer et al., 2002) and has been extensively validated against observations in the past (Vogel et al., 1995; Nester et al., 1995; Fiedler et al., 2000; Corsmeier et al., 2002; Hammer et al., 2002) we only give a short summary with the focus on the aerosol model MADEsoot (Riemer et al., 2003).

In MADEsoot, several overlapping modes represent the aerosol population, which are approximated by log-normal functions. Currently, we use five modes for the submicron particles. Two modes ($\mathbf{i_f}$ and $\mathbf{j_f}$) represent secondary inorganic particles consisting of sulphate, ammonium, nitrate, secondary organic compounds, and water, one mode (**s**) represents pure soot and two more modes ($\mathbf{i_c}$ and $\mathbf{j_c}$) represent particles

ACPD
4, 2089–2115, 2004

consisting of sulphate, ammonium, nitrate, organic compounds, water and soot. The modes $\mathbf{i_f}$, $\mathbf{j_f}$, $\mathbf{i_c}$ and $\mathbf{j_c}$ are assumed to be internally mixed. Thus, the modes $\mathbf{i_f}$ and $\mathbf{j_f}$ represent soot-free particles whereas the modes $\mathbf{i_c}$ and $\mathbf{j_c}$ represent soot containing particles or, in other words, the aged soot particles.

All modes are subject to condensation and coagulation. The growth rate of the particles due to condensation is calculated following Binkowski and Shankar (1995) depending on the available mass of the condensable species (sulphate and organic compounds) and the size distribution of particles. With coagulation, the assignment to the individual modes follows Whitby et al. (1991): (1) Particles formed by intramodal coagulation stay in their original modes. (2) Particles formed by intermodal coagulation are assigned to the mode with the larger median diameter. Furthermore, a thermodynamic equilibrium of gas phase and aerosol phase is applied to calculate the concentrations of sulphate, ammonium, nitrate and water (Kim et al., 1993). The secondary organic compounds are treated according to Schell et al. (2001). The source of the secondary inorganic particles in modes $\mathbf{i_f}$ and $\mathbf{j_f}$ is the binary nucleation of sulphuric acid and water. The soot particles in mode **s** are directly emitted into the atmosphere. The source of the particles in modes $\mathbf{i_c}$ and $\mathbf{j_c}$ is due to the aging process described below. Additionally, sedimentation, advection and turbulent diffusion can modify the aerosol distributions.

In this framework, two processes can impact the transfer of soot from the external into the internal mixture, namely coagulation and condensation. Coagulation of soot particles in mode **s** with particles in modes $\mathbf{i_f}$, $\mathbf{j_f}$, $\mathbf{i_c}$ or $\mathbf{j_c}$ transfers the mass of mode **s** into the modes $\mathbf{i_c}$ or $\mathbf{j_c}$. As a second process, condensation of sulphuric acid on the surface of the soot particles and the formation of ammonium nitrate can transfer soot into an internal mixture as well. Further on at high relative humidity if the aerosol is wet, the nitrate content of the soot aerosol can be increased by the direct solution of HNO_3. To retain the soot mode for pure soot particles, a criteria must be chosen that determines when the aged soot together with the soluble mass is moved to the modes $\mathbf{i_c}$ and $\mathbf{j_c}$. Weingartner et al. (1997) show, that atmospheric particles can be divided into

ACPD
4, 2089–2115, 2004

"more hygroscopic" and "less hygroscopic" depending on their growth behaviour when they are exposed to a relative humidity above 90%. Based on their findings we define that all material of mode **s** is moved to modes $\mathbf{i_c}$ and $\mathbf{j_c}$ if the soluble mass fraction of mode **s** rises above the threshold value ε=5%.

We do not consider the aging process due to photochemical reactions in this study. This is justified since it was shown by Saathoff et al. (2003) that these reactions do not contribute significantly to this process.

We apply the model to an area in southwestern Germany. It covers main parts of Baden-Württemberg and the adjacent regions (248×248 km^2). The horizontal grid size is 4×4 km^2. The biogenic VOC emissions are calculated online depending on the land use, the modeled temperatures and the modeled radiative fluxes (McKeen et al., 1991; Lamb et al., 1987; Vogel et al., 1995). We parameterize the NO emissions from the soil according to Ludwig et al. (2001). The anthropogenic emissions of SO_2, CO, NO_x NH_3, 32 classes of VOC and diesel soot are pre-calculated with the spatial resolution of 4×4 km^2 and a temporal resolution of one hour (Obermeier et al., 1995; Wickert et al., 1999; Pregger et al., 1999; Seier et al., 2000). The diesel soot emissions represent the sources by traffic. In addition to the source strength, we must prescribe the median diameter and the standard deviation of the emitted soot particle distribution. The median diameter is fixed to 60 nm and the standard deviation to 1.8 according to measurements by Vogt et al. (2000).

We investigate two scenarios. First, we simulate a typical summer situation with a geostrophic wind of 4.5 m s^{-1} blowing from East. Second, we consider a winter day with a westerly flow with a geostrophic wind of 4 m s^{-1}. Three consecutive days were simulated in each case.

3. Calculation of the turnover rate

In the following we will explain the approach we use to determine the turnover rate of the externally mixed soot and how this turnover rate can be parameterised for global

climate models. In MADEsoot the temporal development of the mass density $\overline{m}_s$ of the externally mixed soot is determined by the following equation:

$$\frac{\partial \overline{m}_s(\boldsymbol{x},t)}{\partial t} = \overline{A}(\boldsymbol{x},t) + \overline{S}(\boldsymbol{x},t) + \overline{D}(\boldsymbol{x},t) + \overline{E}(\boldsymbol{x},t) - \overline{T}(\boldsymbol{x},t) \quad (1)$$

$\overline{A}$, $\overline{S}$, $\overline{D}$, and $\overline{E}$ describe the rate of change due to advection, sedimentation, turbulent diffusion, and the emission, respectively. The bar indicates that the operators A, S, D and E are applied to the Reynolds-averaged quantities representing a typical spatial and temporal scale. $\overline{T}$ is the turnover rate of the externally mixed soot and the sum of two processes:

$$\overline{T}(\boldsymbol{x},t) = \overline{\mathrm{Ca}}(\boldsymbol{x},t) + \overline{\mathrm{Cn}}(\boldsymbol{x},t) \quad (2)$$

$\overline{\mathrm{Ca}}$ describes the transfer due to the coagulation of the externally mixed soot particles with soot containing internally mixed particles or soot free internally mixed particles. $\overline{\mathrm{Cn}}$ describes the transfer due to condensation of sulphuric acid and organic compounds. The externally mixed soot particles are transferred into internally mixed soot if the soluble mass fraction of mode **s** rises above the threshold value ε=5%. In our mesoscale model system KAMM/DRAIS both processes are explicitly determined as described in Riemer et al. (2003).

Typical applications of the model simulations of KAMM/DRAIS cover areas of about $250\times250\,\mathrm{km}^2$. This equals more or less the typical grid size of a global climate model. In the ideal case averaging a variable over the mesoscale domain A should give the variable of the global climate model (assigned by a tilde).

$$\tilde{a}(z,t) = \frac{1}{A}\iint_A \overline{a}(x,y,z,t)\,dA'. \quad (3)$$

In the global climate model the equivalent equation to Eq. (1) would read as:

$$\frac{\partial \tilde{m}_s(\boldsymbol{x},t)}{\partial t} = \tilde{A}(\boldsymbol{x},t) + \tilde{S}(\boldsymbol{x},t) + \tilde{D}(\boldsymbol{x},t) + \tilde{E}(\boldsymbol{x},t) - \tilde{k}(z,t)\cdot\tilde{m}_s(\boldsymbol{x},t). \quad (4)$$

Here the transfer from the external to the internal mode is already parameterised as a first order reaction since in global climate models the aerosol processes usually cannot be treated as detailed as it is done in regional scale model. The problem is now reduced to the parameterisation of the rate coefficient $\tilde{k}$.

Following the ideas explained so far $\tilde{k}$ can be derived from results of the mesoscale simulations. This means:

$$\tilde{k}(z,t) = \frac{\iint_A \int_{t-\Delta t/2}^{t+\Delta t/2} \overline{T}(x,y,z,t')\, dt'\, dA'}{\iint_A \int_{t-\Delta t/2}^{t+\Delta t/2} \overline{m}_s(x,y,z,t')\, dt'\, dA'}. \quad (5)$$

with Δt=1 h. This time interval was chosen as it is comparable to the time steps that are used in global climate models. In this way we determine time-dependent vertical profiles of $\tilde{k}$. The timescale $\tau(z,t)$ that represents the exponential timescale for the decay of externally mixed soot is given by

$$\tau(z,t) = \frac{1}{\tilde{k}(z,t)}. \quad (6)$$

4. Results

Figures 1 and 2 show the horizontal distributions of the soot concentration in external and internal mixtures at 20 m above the surface at 12:00 CET (day 2) for the summer and the winter episode. The distributions of the soot in external mixture reflect the distribution of the sources, i.e. the main motorways and urban centres in the model domain. In the plumes of the urban areas and at some distance from the sources, soot is internally mixed. Comparing the winter and summer results we find that the total soot concentrations reach significantly higher values in winter due to the shallower boundary layer and the reduced vertical mixing in winter.

ACPD
4, 2089–2115, 2004

Figures 3 and 4 show the vertical cross sections of the soot concentration at y=80 km for the summer case. In the elevated layers soot exists mainly internally mixed. The values for the total soot concentrations range between 0.1 and 2 $\mu g\,m^{-3}$ near the surface at 12:00 CET (day 2). However, higher concentrations (up to 10 $\mu g\,m^{-3}$) are reached in the morning hours.

On the basis of the simulation results for both episodes we derive the aging timescale τ as described in Sect. 3. As explained there, τ may depend on height and time. Figure 5 shows time height sections of τ for the summer and winter episode, respectively. In both cases τ is below 2 h during the day and above 250 m above the surface. During the same time interval and below this height τ varies between 1 hour during the morning and up to about 20 h in the afternoon. During night time τ is much larger than during the day at all heights and there is a strong increase of τ from midnight of day 2 to midnight of day 3 in the summer and the winter case. While τ is almost constant with height during the night in the summer case it decreases with height in the winter case. Considering the temporal and spatial variations of τ in Fig. 5, it becomes obvious that the parameterisation of the aging process of soot using a fixed turnover rate represents an oversimplification.

Figure 6a displays the daily cycle of τ in three different heights within the boundary layer for the summer episode (day 2) in more detail. At the heights of 250 m and 1100 m, we can clearly distinguish between the daytime and the night time regime. During daytime at these heights, τ is very short (~1 h). From detailed process studies based on our model results we find that condensation is very efficient in transferring externally mixed soot into the internal mixture when sulphuric acid is abundant. During the night, the production of sulphuric acid ceases. Once the available sulphuric acid has been depleted by condensation on the existing particles, condensation therefore stops to occur. Under these conditions coagulation is the only process for the transfer into internal mixture, operating very slowly. This leads to much higher values for τ during the night compared to the day.

At the height of 25 m, which is identical with the source height used for our simula-

tions, the distinction between day and night is not as apparent and τ remains at a relatively high level of about 20 h in the afternoon. The reason is that at this height, fresh soot is permanently emitted and the concentration of externally mixed soot reaches its maximum. Given a certain amount of condensable species, it takes a longer time until the shell mass has grown to the certain threshold that marks the transition between externally and internally mixed soot which eventually results in the high values for τ.

At all heights a characteristic trend of the timescale is obvious. This trend can be attributed to the fact that the coagulation rate depends on the particles number densities. The particle number densities of the mode **s** are largely dominated by the emissions. However, the number densities of the modes $\mathbf{i_f}$, $\mathbf{j_f}$, $\mathbf{i_c}$ and $\mathbf{j_c}$ are decreasing with time in our simulation, because nucleation on the third day is weaker than on the second day due to the meteorological conditions. Consequently, since these are the particles that provide the coagulation partner for the externally mixed soot for the transfer into the internal mixture, the timescale τ increases.

Similar arguments apply to the winter episode as displayed in Fig. 6b. Compared to the summer conditions, however, important differences concern the following issues: Obviously, the daytime is shorter, solar radiation less intense and temperatures are significantly lower. This causes a shallower boundary layer and decelerated photochemistry, in particular a lower production rate of H_2SO_4. However, the lower temperatures favour the formation of ammonium nitrate. It turns out that ammonium nitrate contributes significantly to the aging of soot in winter and hence compensates the lack of H_2SO_4 leading to time scales during the day that are comparable to the summer case. To underline these findings, Fig. 7 shows the average mass densities of the individual species for the internally mixed soot aerosol at 12:00 CET (day 2) at 25 m above the surface. While the soluble mass fraction of these aerosol particles is clearly dominated by sulphate for the summer case nitrate represents the main contribution for the winter case.

The pronounced minimum for the time scale in 25 m (Fig. 6b) can be attributed to the interaction of two processes that act in the opposite direction: First, the formation

ACPD
4, 2089–2115, 2004

of ammonium nitrate sets in, which leads to a decrease in τ. Concurrently, the surface area of the particles in the modes $\mathbf{i_f}$, $\mathbf{j_f}$, $\mathbf{i_c}$ and $\mathbf{j_c}$ increases compared to the surface of the particles in mode **s**. Therefore the low value of τ cannot be sustained and increases again. For the development of a parameterisation, we will neglect this feature in order to keep the parameterisation as simple as possible.

5. Parameterisation of τ for global climate models

Based on our model results we will now develop a parameterisation of the aging process of soot particles which can be applied in global climate models to replace the assumption of a single and constant aging time scale used in previous studies (Cooke et al., 1996; Lohmann et al., 2000). We propose to use this parameterisation for global climate models for industrialised areas where continental conditions apply.

Although detailed aerosol models comparable to MADEsoot have been used in global scale models to treat the aging process explicitly (Wilson et al., 2001) there is a still a need for such parameterisations. If such a global model runs in the climate mode for simulation times of several hundred of years it is still necessary to replace detailed physical descriptions by parameterisations.

Coagulation, condensation and heterogeneous chemistry are very complex processes. Since we nevertheless intend to develop a rather simple parameterisation we cannot expect that this parameterisation describes every detail of the exact processes. The availability of the variables within the global climate model determines the degree of simplicity of the parameterisation. The mass density of the externally mixed soot and the number density of the internally mixed particles usually are amongst these variables.

One possibility would be to parameterise the aging of the soot aerosol based on the production rate of H_2SO_4 since the condensation of sulphuric acid initializes the aging of the soot particles. However, by doing so one would obtain rather long lifetimes during winter when the solar flux is low and consequently the sulphate production is

ACPD
4, 2089–2115, 2004

small. This contradicts our findings. As we have seen for the winter conditions, it shows that although the aging process of the soot particles starts with condensation of H_2SO_4 the mass fraction of sulphate on the soot particles is rather low but the nitrate content is high. Hence, when low temperatures and low solar flux prevail, the formation of nitrate on the aerosol determines the aging timescale. Therefore we propose the following parameterisation. We separate between daytime and night time conditions (Fig. 8). The separation bases on the global radiation at the surface. During daytime we additionally distinguish between the layers above 250 m and the layers below this height. These distinctions are used regardless of the season.

During daytime and above 250 m above the surface τ is approximately 2 h. In order to derive the timescale during daytime and below 250 m we apply the following procedure. The timescales shown in Fig. 5 are averaged below 250 m and for the time interval where the global radiation is above zero. We find an average timescale of 9.38 h for the summer case and 6.89 h for the winter case. In order to use a single number independent of the season for this height interval we propose to use 8 h for the aging timescale.

For the parameterisation of the night time conditions we assume that $\tilde{k}$ and τ depend only on the number density of the internally mixed particles (that is the particles in the modes $\mathbf{i_f}$, $\mathbf{j_f}$, $\mathbf{i_c}$ and $\mathbf{j_c}$). Of course this is a rather crude approximation since the coagulation depends on the number densities, the mean diameters, the coagulation coefficients and other parameters e.g. the temperature. Figure 9 shows the simulated values of τ versus the number density of the internally mixed particles for the summer days and the winter days. All grid points are shown for heights below 1100 m above the surface during night time. As expected a decrease of τ with increasing number density is obvious. For these data we calculate two non-linear fits, the results of which are depicted in Fig. 9. We find the following relations:

$$\tau = \exp\ (-a \cdot N + b) \tag{7}$$

ACPD
4, 2089–2115, 2004

with $a = 2.3012 \cdot 10^{-4} \cdot \mathrm{cm}^3$ and $b = 4.4428$.

$$\tau = -c + d \cdot N^{-1} \quad (8)$$

with $c = 3.8585$ h and $d = 1.48 \cdot 10^5$ h cm^{-3}.

N is the number density in the modes $\mathbf{i_f}$, $\mathbf{j_f}$, $\mathbf{i_c}$ and $\mathbf{j_c}$ in cm^{-3} and the dimension of τ is h in both cases.

In the number density range between 3000 and 9000 particles cm^{-3} both fits give almost identical results. The fit according to Eq. (7) fails for particle number concentrations close to zero since in this case τ should reach infinity. The fit according to Eq. (8) fails for particle number concentrations approximating infinity since in this case τ should be equal to zero. Therefore, for practical use in a global climate model we propose to use Eq. (7) for particle number densities less than 4100 cm^{-3} and Eq. (8) for particle number densities greater than 4100 cm^{-3}.

Obviously, approximating τ by Eqs. (7) and (8) has a shortcoming. The data for both simulations show a lot of scatter, especially for the low number densities, which is mainly caused by the height dependency of the timescale. This means we find different timescales for the same number density at different heights. This problem could be overcome by grouping the data points with respect to height and deriving individual fits for each height. However, we doubt that this would increase the accuracy of our parameterisation. We think that it is rather more important to take into account the variation of τ with the number density of the particles than taking into account the variation of τ with height at a given number density. For this reason we propose to use Eqs. (7) and (8) independent of height. In any case the parameterisation proposed here represents a major improvement over the use of only one constant value for the transfer rate $\tilde{k}$ as it is the current practice.

Another shortcoming of our parameterisation is that we studied two situations only. Of course it would be better to increase the number of realisations. Nevertheless, we have shown that during night time coagulation limits the aging timescale. Therefore, we do not expect different results by increasing the number of cases. Concerning daytime

conditions, when condensation limits the aging timescale, it is important to take into account the winter and the summer case, because the composition of the particles differs tremendously. Since we find in both cases very low and similar timescales above 250 m above the surface as well as below this height we expect our findings are rather robust. Nevertheless, they have to be confirmed by further studies.

6. Conclusions

We performed three-dimensional model simulations with the coupled mesoscale-γ model KAMM/DRAIS to derive the timescale τ that characterizes the transfer of diesel soot from external into internal mixture as would be used in a global climate model. Since our model simulations represent continental conditions in an industrialised area, we want to limit our parameterisation accordingly to these conditions.

Generally, the aging timescales that we derived are smaller than most of the values that are currently used in global climate models. During daytime in summer, condensation of sulphuric acid is the governing process for the aging of soot. In wintertime, the formation of ammonium nitrate gains in importance. Overall, the timescales for daytime in summer and winter are comparable. During night time, condensation stops being the important process. Instead, coagulation becomes more significant, acting very slowly.

Based on our model results we conclude with the following recommendations:

For daytime conditions and above 250 m the aging process occurs very fast. We suggest a value of τ=2 h. Below this height and during daytime we propose to use τ=8 h. During night time, condensation is not effective; therefore the parameterisation according to Eqs. (7) and (8) must be applied. This leads to a timescale between 10 h and 40 h.

ACPD
4, 2089–2115, 2004

References

Baltensperger, U., Streit, N., Weingartner, E., Nyeki, S., Prévôt, A. S. H., Van Dingenen, R., Virkkula, A., Putaud, J.-P., Even, A., ten Brink, H., Blatter, A., Neftel, A., and Gäggeler, H. W.: Urban and rural aerosol characterization of summer smog events during the PIPAPO field campaign in Milan, Italy, J. Geophys. Res., 107, 8193 doi:10.1029/2001JD001292, 2002.

Binkowski, F. S. and Shankar, U.: The regional particulate matter model, 1. Model description and preliminary results, J. Geophys. Res., 100, 26 191–26 209, 1995.

Brémond, M.-P., Cachier, H., and Buat-Ménard, P.: Particulate carbon in the Paris region atmosphere, Environ. Technol. Lett., 10, 339–346, 1989.

Cooke, W. F. and Wilson, J. N.: A global black carbon aerosol model, J. Geophys. Res., 101, 19 395–19 408, 1996.

Cooke, W. F., Liousse, C., Cachier, H., and Feichter, J.: Construction of a 1°×1° fossil fuel emission data set for carbonaceous aerosol and implementation and radiative impact in the ECHAM4 model, J. Geophys. Res., 104, 22 137–22 162, 1999.

Corsmeier, U., Kalthoff, N., Vogel, B., Hammer M.-U., Fiedler F., Kottmeier C., Volz-Thomas A., Konrad S., Glaser K., Neininger B., Lehning M., Jaeschke W., Memmesheimer M., Rappenglück B., and Jakobi, G.: Ozone and PAN formation inside and outside of the Berlin plume – Process analysis and numerical process simulation, J. Atmos. Chem., 42, 289–322, 2002.

Fiedler, F.; Bischoff-Gauß, I.; Kalthoff, N.; and Adrian, G.: Modeling of the transport and diffusion of a tracer in the Freiburg-Schauinsland area, J. Geophys. Res., 105, 1599–1610, 2000

Hammer, M.-U., Vogel, B., and Vogel, H.: Findings on H_2O_2/HNO_3 as an indicator of ozone sensitivity in Baden-Württemberg, Berlin-Brandenburg, and the Po valley based on numerical simulations, J. Geophys. Res., 107, 8190, doi:10.1029/2000JD000211, 2002.

Heintzenberg, J.: A processor-controlled multisample soot photometer, Aerosol Sci. Technol., 8, 227–233, 1988.

Horvath, H.: Atmospheric light absorption – A review, Atmos. Environ., 27, 293–317, 1993.

Jacobson, M. Z.: A physically based treatment of elemental carbon optics: Implications or global direct forcing of aerosols, Geophys. Res. Lett., 27, 217–220, 2000.

Jacobson, M. Z.: Control of fossil-fuel particulate black carbon and organic matter, possibly the most effective method of slowing global warming, J. Geophys. Res., 107, 4410,

doi:10.1029/2001JD001376, 2002.
Kim, Y. P., Seinfeld, J. H., and Saxena, P.: Atmospheric gas-aerosol equilibrium I. Thermodynamic model, Aerosol Sci. Technol., 19, 157–181, 1993.
Koch, D.: Transport and direct radiative forcing of carbonaceous and sulfate aerosols in the GISS GCM, J. Geophys. Res., 106, 20 311–20 332, 2001.
Lamb, B., Guenther, A., Gay, D., and Westberg, H.: A national inventory of biogenic hydrocarbon emissions, Atmos. Environ., 21, 1695–1705, 1987.
Lesins, G., Chylek, P., and Lohmann, U.: A study of internal and external mixing scenarios and its effect on aerosol optic properties and direct radiative forcing, J. Geophys. Res., 107, 4094, doi:10.1029/2001JD000973, 2002.
Liousse, C., Penner, J.E., Chuang, C., Walton, J.J., Eddleman, H., and Cachier, H.: A global tree-dimensional model study of carbonaceous aerosols, J. Geophys. Res., 101, 19 411–19 432, 1996.
Lohmann, U., Feichter, J., Penner, J., and Leaitch, R.: Indirect effect of sulfate and carbonaceous aerosols: A mechanistic treatment, J. Geophys. Res., 105, 12 193–12 206, 2000.
Ludwig, J., Meixner, F.X., Vogel, B., and Förstner, J.: Soil-air exchange of nitric oxide: An overview of processes, environmental factors, and modeling studies, Biogeochemistry, 52, 225–258, 2001.
McKeen, S. A., Hsie, E.-Y., and Liu, S. C.: A study of the dependence of rural ozone on ozone precursors in the eastern United States, J. Geophys. Res., 96, 15 377–15 394, 1991.
Myhre, G., Stordal, F., Restad, K., and Isaksen I. S. A.: Estimation of the direct radiative forcing due to sulfate and soot aerosol, Tellus, 50B, 463–477, 1998.
Nester, K., Panitz, H.-J., and Fiedler, F.: Comparison of the DRAIS and EURAD model simulations of air pollution in a mesoscale area, Meteorol. Atmos. Phys., 57, 135–158, 1995.
Nenes, A., Conant, W. C., and Seinfeld, J. H.: Black carbon radiative heating effects on cloud microphysics and implications for the aerosol indirect effect – 2. Cloud microphysics, J. Geophys. Res., 107, 4605, doi:10.1029/2002JD002101, 2002.
Obermeier, A., Friedrich, R., John, C., Seier, J., Vogel, H., Fiedler, F., and Vogel, B.: Photosmog: Möglichkeiten und Strategien zur Verminderung des bodennahen Ozons, Umweltforschung in Baden-Württemberg, ecomed Verlagsgesellschaft, Landsberg, 1995.
Okada, K. and Hitzenberger, R. M.: Mixing properties of individual submicrometer aerosol particles in Vienna, Atmos. Environ., 35, 5617–5628, 2001.
Pope, A. and Dockery, D.: Epidemiology of chronic health effects: Cross-sectional studies, in:

Particles in Our Air: Concentrations and Health Effects, edited by Wilson, R., and Sprengler, J., Cambridge, MA, Havard University Press, 149–168, 1996.

Pregger, T., Friedrich, R., Obermeier, A., Wickert, B., Blank, P., Theloke, J., Vogel, H., Riemer, N., Vogel, B., and Fiedler, F.: Entwicklung von Instrumenten zur Analyse der Umweltbelastungen durch Feinstäube und andere ausgewählte Luftverunreinigungen in Baden-Württemberg, http://bwplus.fzk.de, 1999.

Riemer, N., Vogel H., Vogel, B., and Fiedler F.: Modeling aerosols on the mesoscale-γ: Treatment of soot aerosol and its radiative effects, J. Geophys. Res., 109, 4601, doi: 10.1029/2003JD003448, 2003.

Saathoff, H., Naumann, K.-H., Riemer, N., Kamm, S., Möhler, O., Schurath, U., Vogel, H., and Vogel, B.: The loss of NO_2, HNO_3, NO_3/N_2O_5, $HO_2/HOONO_2$ on soot aerosol: A chamber and modeling study, Geophys. Res. Lett., 28, 1957–1960, 2001.

Saathoff, H., Naumann, K. H., Schnaiter, M., Schöck, W., Möhler, O., Schurath, U., Weingartner, E., Gysel, M., and Baltensperger, U.: Coating of soot and $(NH_4)_2SO_4$ particles by ozonolysis products of α-pinene. J. Aerosol Sci., 34, 1297–1321, doi:10.1016/S0021-8502(03)00364-1, 2003.

Schell, B., Ackermann I. J., Binkowski, F. S., and Ebel, A.: Modeling the formation of secondary organic aerosol within a comprehensive air quality model system, J. Geophys. Res., 106, 28 275–28 293, 2001.

Seier, J., Berner, P., Friedrich, R., John, C., and Obermeier, A.: Generation of an emission data base for TRACT, in: Exchange and Transport of Air Pollutants over Complex Terrain and the Sea, edited by Larsen, S., Fiedler, F., and Borell, P., Springer Verlag, Berlin, Heidelberg, 269–278, 2000.

Tsigaridis, K. and Kanakidou, M.: Global modeling of secondary organic aerosol in the troposphere: A sensitivity analysis, Atmos. Chem. Phys. Discuss., 3, 2879–2929, 2003.

Vogel, B., Fiedler, F., and Vogel, H.: Influence of topography and biogenic volatile organic compounds emission in the state of Baden-Württemberg on ozone concentrations during episodes of high air temperatures, J. Geophys. Res., 100, 22 907–22 928, 1995.

Vogt, R., Scheer, V., and Rehbein, C.: Measurement of exhaust particles: A comparison of the Emission lab and atmosphere, Contribution at IAA Technical Congress, Frankfurt, 2000.

Weingartner, E., Burtscher, H., and Baltensperger, H.: Hygroscopic properties of carbon and diesel soot particles, Atmos. Environ., 31, 2311–2327, 1997.

Whitby, E. R., McMurray, P. H., Shankar, U., and Binkowski, F. S.: Modal Aerosol Dynamics

Modeling, Atmos. Res. and Exposure Assess. Lab. U.S. Environ. Prot. Agency, 600/3-91/020, (NTIS PB91-161729/AS Natl. Tech. Inf. Serv. Springfield, Va.), Research Triangle Park, N.C, 1991.

Wickert, B., Schwarz, U., Blank, P., John, C., Kühlwein, J., Obermeier, A., and Friedrich, R., Generation of an emission data base for Europe 1994, in Proceedings of EUROTRAC Symposium'98, edited by Borrell, P. M. and Borrell, P., WITPress, Boston, Southampton, 2, 255–260, 1999.

Wilson, J., Cuvelier, C., and Raes, F.: A modeling study of global mixed aerosol fields, J. Geophys. Res., 106, 34 081–34 108, 2001.

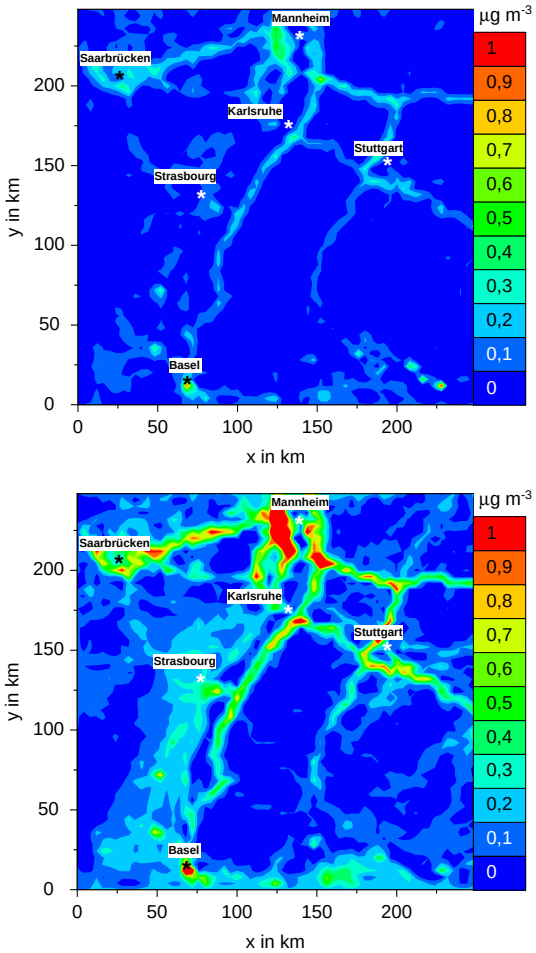

Fig. 1. Horizontal distribution of the externally mixed soot at 20 m above the surface, 12:00 CET, day 2 (top: summer, bottom: winter).

ACPD

4, 2089–2115, 2004

A parameterisation of the soot aging

N. Riemer et al.

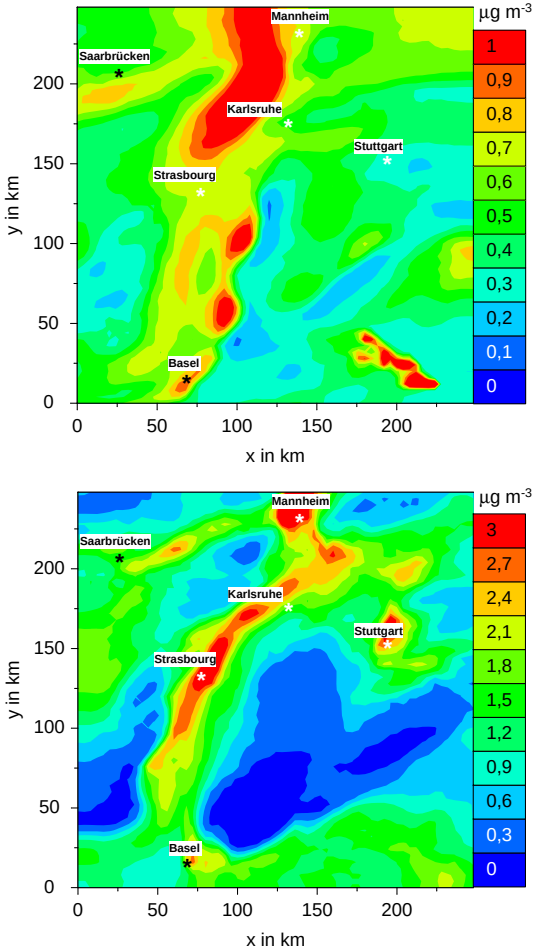

Fig. 2. Same as Fig. 1, but for internally mixed soot.

ACPD
4, 2089–2115, 2004

A parameterisation of the soot aging

N. Riemer et al.

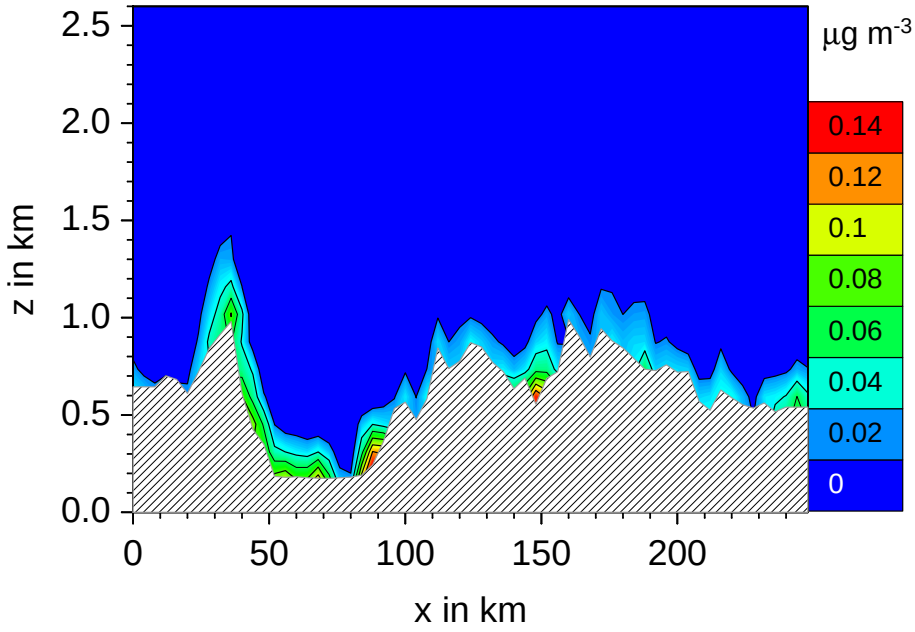

Fig. 3. Vertical cross section of the externally mixed soot concentration for the summer case at y=80 km, 12:00 CET, day 2.

ACPD
4, 2089–2115, 2004

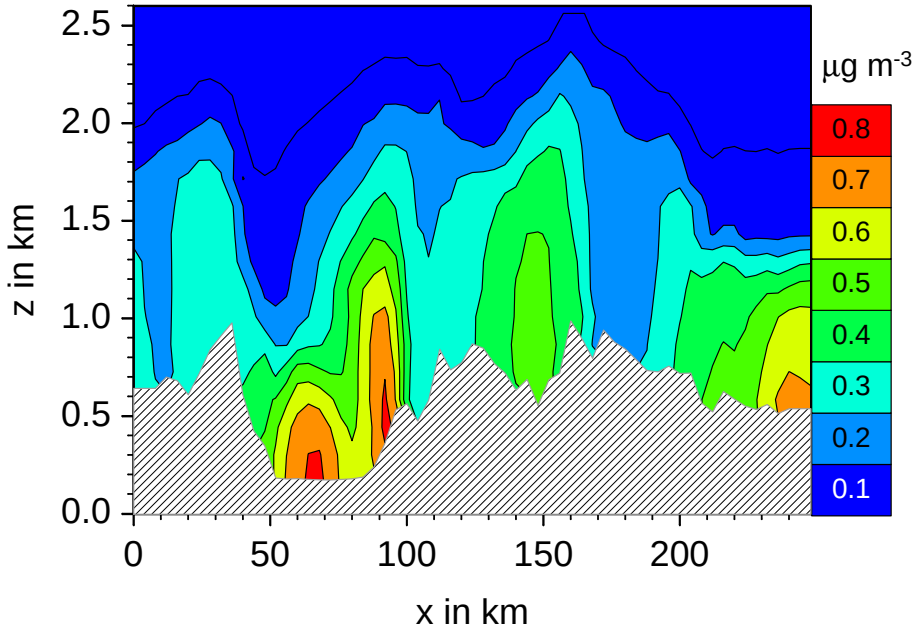

Fig. 4. Same as Fig. 3, but for internally mixed soot.

ACPD
4, 2089–2115, 2004

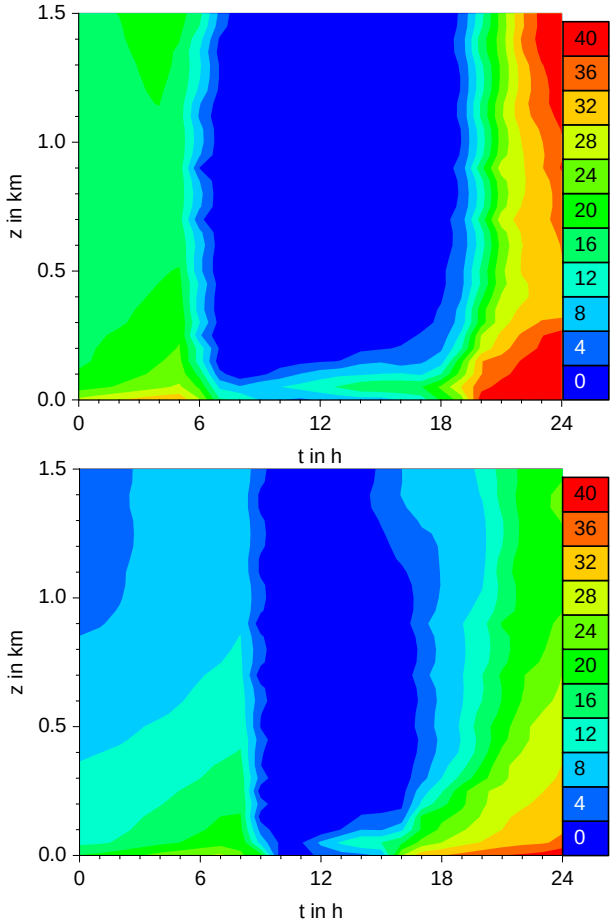

Fig. 5. Vertical profiles for the aging timescale for summer (top) and winter (bottom) at day 2.

ACPD
4, 2089–2115, 2004

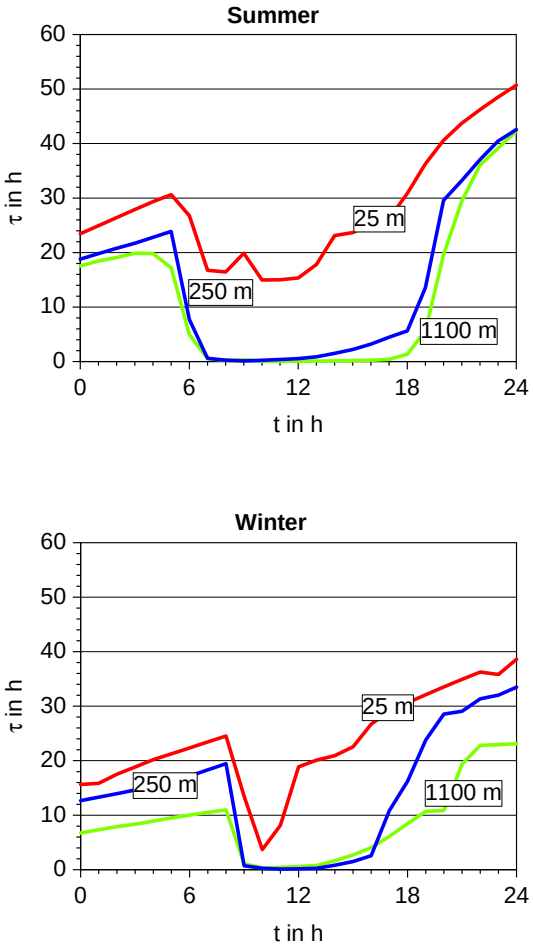

Fig. 6. Daily cycles of the aging timescale (day 2).

ACPD
4, 2089–2115, 2004

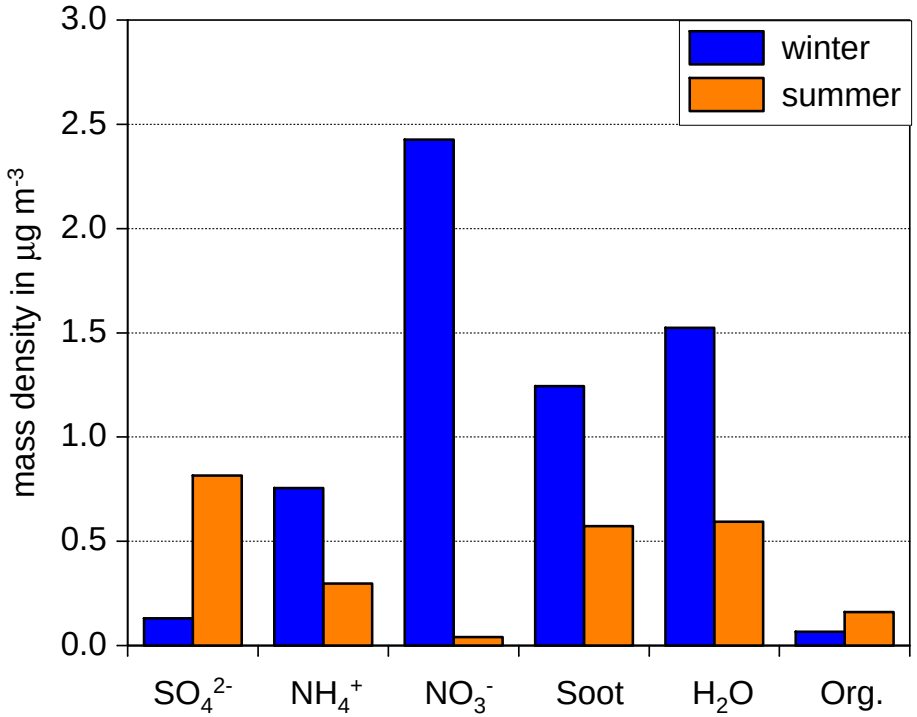

Fig. 7. Composition of the internally mixed soot particles at 14:00 CET at 25 m above the surface.

ACPD
4, 2089–2115, 2004

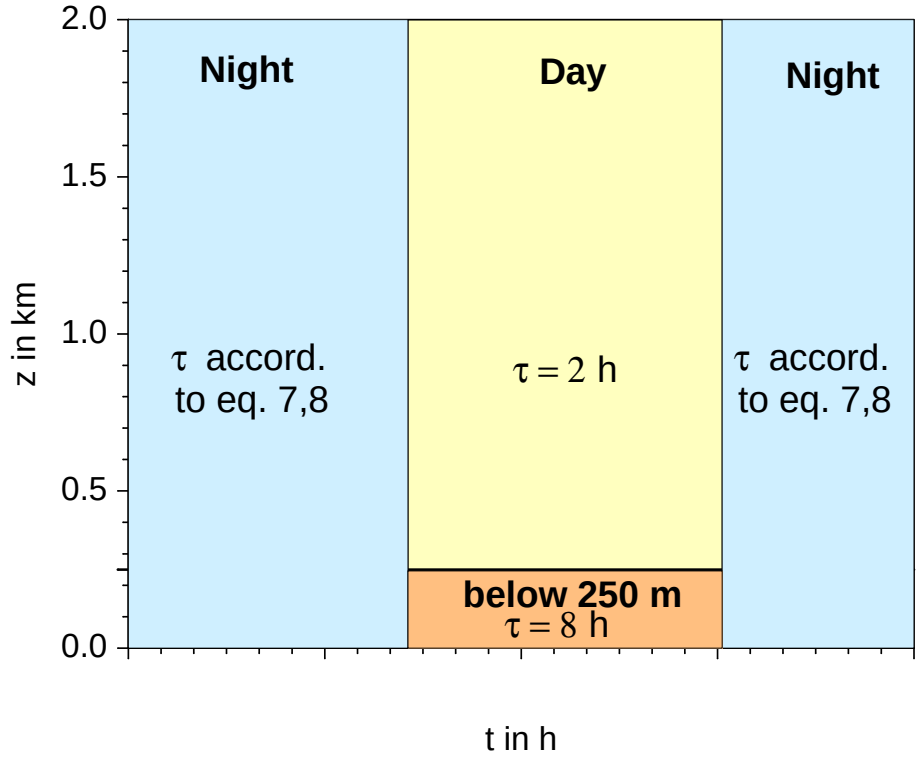

Fig. 8. Sketch to distinguish the time height zones for the parameterisation.

ACPD
4, 2089–2115, 2004

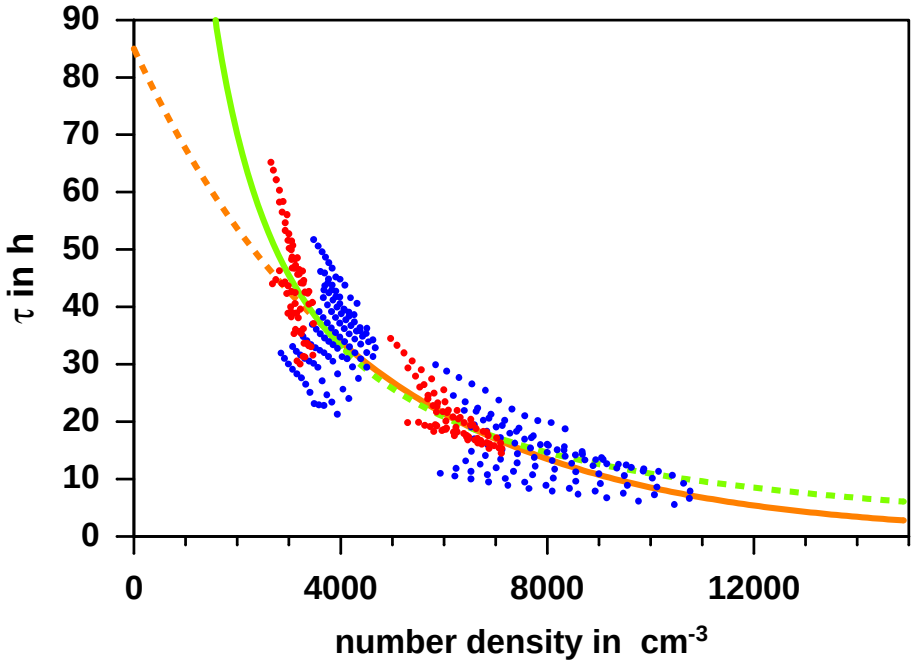

Fig. 9. Correlation of τ and the number density of the internally mixed particles. The solid lines show the fits based on the winter day. The blue dots indicate the results for the winter day, the red ones those for the summer day. The orange line gives τ according to Eq. (7), the green line gives τ according to Eq. (8).

ACPD
4, 2089–2115, 2004